

FRACTAL BASINS OF ATTRACTION IN A BINARY QUASAR MODEL

Vinay Kumar

*Department of Mathematics, Zakir Husain Delhi College,
University of Delhi, Delhi, India
email: vkumar@zh.du.ac.in*

Pankaj Sharma

*Department of Mathematics, Zakir Husain Delhi College,
University of Delhi, Delhi, India
drps4m@gmail.com*

Rajiv Aggarwal

*Department of Mathematics, Sri Aurobindo College,
University of Delhi, Delhi, India
rajiv_agg1973@yahoo.com*

Bhavneet Kaur

*Department of Mathematics, Lady Sri Ram College,
University of Delhi, Delhi, India
bhavneet.lsr@gmail.com*

Received xxxxxxxx

The present paper investigates the binary system of quasars in the framework of the Circular Restricted Three-Body Problem. The parametric evolution of libration points, the geometry of zero-velocity curves are one of the crucial aspects of our study. The multivariate form of NR method is applied to study the basin of attraction connected with libration points. The algorithm for using the Newton-Raphson method is slightly modified in order to avoid the unnecessary delay in the convergence of initial conditions. The impact of parameters on the shape of the basin of attraction and the number of iterations needed for the convergence of initial conditions are explored. We carry out an exhaustive (numerical) study to show the influence of these parameters on converging regions in basins of convergence. We unveil the existence of fractal structure in the basin of attraction using the method of basin entropy. In almost all cases, the existence of fractal structure is found throughout the basins of attraction.

Keywords: Basins of convergence(BoC), Basin Entropy, Newton-Raphson Method(NR-method), Binary System of Interacting Galaxies, fractal region

1. Introduction

The study of the complexity of the phase space of nonlinear models in the field of space dynamics and celestial mechanics have gained considerable attention nowadays. Mathematicians who have been working

in this field for decades are trying to explore several nonlinear models. They have introduced many tools to study the phase space structure of these models. The basins of attraction (BoA)(or basin of convergence (BoC)) are one of the essential tools. Our observations took place while following many recent contributions in this field such as [Zotos, 2017], [Suraj, 2019] and [Zotos, 2018]. The study of BoA reveals the regions of initial conditions which converges smoothly towards libration points of the system under consideration. However, there are regions of initial conditions which creates an obstacle for smooth convergence. It is because of the non-linearity that existed in the equations of motion for a particular system under consideration.

The galactic model that has been considered in our work is the system of binary quasars. We have studied this model under the assumption of Circular Restricted Three-Body Problem (CRTBP). In [Zotos, 2012] and [Kumar, 2016], one can observe the applications of the Poincaré section, the method of Lyapunov exponents and wavelet transform method to understand the phase space of this model. The first time, through this work, we have investigated the BoA in the model of spaces of galaxies. In the recent past few researchers are working in these models and trying to explore the dynamics of this model. In continuation of that, we have also deliberated the parametric evolution of libration points in the value of parameters as well as the zero-velocity curves.

However, it is not easy to establish the existence of fractal structure in general. Recently, Alvar Daza [Alvar, 2016] has introduced the concept of basin entropy to show the existence of fractals in BoA. Some applications of this method can also be seen in the work of [Alvar, 2017], [Alvar, 2018]. The method of basin entropy is the quantification of uncertainty involved in BoA. We compute the basin entropy S_b and entropy along the boundaries S_{bb} of the BoA. If the value of S_b or S_{bb} is greater than $\log 2$, then BoA or boundaries along the BoA is fractal. We choose this method to reveal the existence of fractals connected with libration points of the binary system of interacting galaxies.

Further, we have noticed several numerical methods while studying the BoA. Some notable works have been observed in the work of [Zotos, 2017], [Suraj, 2019] and [Zotos, 2018]. From results established in these papers, we notice that the NR-method is efficient to study in such a phenomenon. Therefore, we have considered the multivariate NR-method to study the convergence of BoA.

The present paper aims to study the BoA in the system of binary quasars. Also, we have tried to investigate the existence of fractal. We have applied the multivariate NR-method and the method of basin entropy. The algorithm for finding BoA is written in such a way that it excludes unnecessary iteration time consumed by CPU.

The organisation of the present work is as follows: In Section 2, the configuration of a binary quasar model is described. The parametric evolution of the libration points and the geometry of zero-velocity curves under the effect of parameters are included in its subsections. The Newton–Raphson Method and the recently developed tool basin entropy are explained in Section 3. Section 4 comprises the results and discussion and finally, we have made concluding remarks related to the observations based on numerical simulations in Section 5.

2. Configuration of binary quasar model

The binary quasars is the system of interacting galaxies, which are bound together by gravitational forces. It is believed to be the product of the merger of galaxies. At present, it is known that many interacting quasars are hold in massive spiral galaxies with prominent disks [Latewe, 2007]. To date (to the best of our knowledge) OJ287 [Sillianpaa et al., 1988] is the famous close binary pair of supermassive black holes (SMBH). Our model contains a pair of disk galaxies equipped with a dense, massive and spherically symmetric nucleus. Notably, the potential which governs the motion of a star due to the first galaxy (G_1) is expressed as:

$$V_1(r, z) = V_{n1}(r, z) + V_{d1}(r, z) = -\frac{M_{n1}}{\sqrt{r^2 + z^2 + c_{n1}^2}} - \frac{M_{d1}}{\sqrt{b_1^2 + r^2 + \left(a_1 + \sqrt{h_1^2 + z^2}\right)^2}}, \quad (1)$$

where $r^2 = x^2 + y^2$. The galaxy has mass on the disk M_{d1} and the mass on the nucleus is M_{n1} . a_1 and h_1 are the scale length and scale height of the disk respectively. The core radius of the disk halo is b_1 and

c_{n1} is the scale length of the nucleus.

Similarly, the potential accountable for the motion of the star due to G2 is expressed as

$$V_2(r, z) = V_{n2}(r, z) + V_{d2}(r, z) = -\frac{M_{n2}}{\sqrt{r^2 + z^2 + c_{n2}^2}} - \frac{M_{d2}}{\sqrt{b_2^2 + r^2 + \left(a_2 + \sqrt{(h_2)^2 + z^2}\right)^2}}, \quad (2)$$

The galaxy has mass on the disk M_{d2} and the mass on the nucleus is M_{n2} . a_2 and h_2 are the scale length and scale height of the disk respectively. The core radius of the disk halo is b_2 and c_{n2} is the scale length of the nucleus.

Expressions for the disk of host galaxies are taken from the work of Miyamoto-Nagai [Miyamoto and Nagai, 1975] and [Zotos, 2012]. We have considered the Plummer sphere to express the nuclei of both galaxies [Hasan et al., 1993]. In this model, we study the motion of a star under the influence of the binary quasars in the framework of the CRTBP. The two galaxies rotate in circular orbits in an inertial frame OXYZ, with the origin at the centre of mass of the system with a constant angular velocity

$$\Omega_p = \sqrt{\frac{GM_t}{R^3}} > 0 \quad (3)$$

where $M_t = M_{n1} + M_{d1} + M_{n2} + M_{d2}$. Here, the total mass of the system is M_t and the distance between the centers of two galaxies is R . Also, the frame which is rotating with angular velocity Ω_p has fixed positions at $C_1(x, y, z) = (x_1, 0, 0)$ and $C_2(x, y, z) = (x_2, 0, 0)$, respectively. The distance between two interacting galaxies is such that the tidal forces are very small and can be neglected. Therefore, the net potential accountable for the motion of a star in the Binary Quasar System is

$$\phi_t(x, y, z) = \phi_{G1}(x, y, z) + \phi_{G2}(x, y, z) + \phi_{rot}(x, y, z), \quad (4)$$

where

$$\phi_{G1}(x, y, z) = -\frac{M_{n1}}{\sqrt{r_1^2 + c_{n1}^2}} - \frac{M_{d1}}{\sqrt{b_1^2 + r_{a1}^2 + \left(a_1 + \sqrt{h_1^2 + z^2}\right)^2}}, \quad (5)$$

$$\phi_{G2}(x, y, z) = -\frac{M_{n2}}{\sqrt{r_2^2 + c_{n2}^2}} - \frac{M_{d2}}{\sqrt{b_2^2 + r_{a2}^2 + \left(a_2 + \sqrt{h_2^2 + z^2}\right)^2}}, \quad (6)$$

$$\phi_{rot}(x, y) = -\frac{\Omega_p^2}{2} \left(\frac{M_2}{M_t} r_{a2}^2 + R_s r_{a1}^2 - R^2 \frac{M_2}{M_t} R_s \right) \quad (7)$$

$$(r_{a1})^2 = (x - x_1)^2 + y^2, \quad (r_{a2})^2 = (x - x_2)^2 + y^2, \quad (r_1)^2 = (r_{a1})^2 + z^2, \quad (r_2)^2 = (r_{a2})^2 + z^2,$$

$$x_1 = -\frac{M_2}{M_t} R, \quad x_2 = R - \frac{M_2}{M_t}, \quad M_2 = M_{n2} + M_{d2}, \quad R_s = 1 - \frac{M_2}{M_t}.$$

In synodic frame the equations of motions (two dimension) are,

$$\ddot{x} = -\frac{\partial \phi_t}{\partial x} - 2\Omega_p \dot{y} \quad \ddot{y} = -\frac{\partial \phi_t}{\partial y} - 2\Omega_p \dot{x}. \quad (8)$$

The Jacobi integral for the system of equations of motion (8) is given by the equation

$$J = \frac{1}{2} (\dot{x}^2 + \dot{y}^2) + \phi_t(x, y) = E_j, \quad (9)$$

where \dot{x} , \dot{y} and \dot{z} are the momenta corresponding to coordinates x , y and z respectively. We use the following galactic units:

- Unit of length is 20 kiloparsec (one parsec $\simeq 3.26$ light years).
- Unit of mass is $1.8 \times 10^{11} M_{\odot}$ (M_{\odot} denotes the solar mass which is equal to $1.98892 \times 10^{30} kg$).
- Unit of time is 0.99×10^8 year.
- Unit of velocity is 197 km/sec.
- $G=1$.

In these units, we use $a_1 = 0.15, b_1 = 0.2542, h_1 = 0.00925, c_{n1} = 0.0125, c_{n1} = 0.0125, a_2 = 0.175, b_2 = 0.0789, h_2 = 0.00875$ and $c_{n2} = 0.01$, which remain constant throughout the computations. The values of $M_{n1}, M_{d1}, M_{n2}, M_{d2}$ and R are parameters. [Zotos, 2012]

2.1. Influence on libration points due to variation in parameters

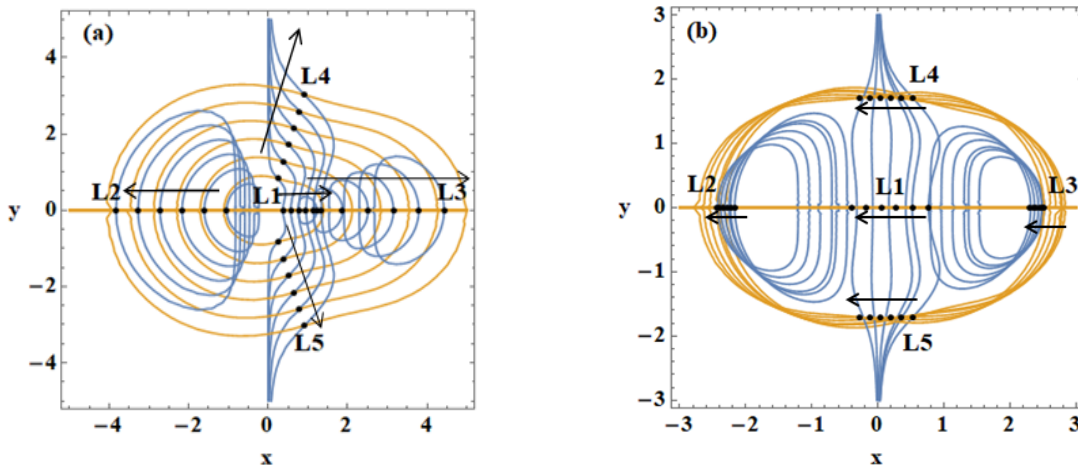


Fig. 1. (a) Movement of libration points due to variation in R , (b) Movement of libration points due to variation in M_{n1}, M_{d1}, M_{n2} and M_{d2} .

In Fig.1(a) and Fig.1(b), we have presented the effect of parameter R and effect of parameters $M_{n1}, M_{d1}, M_{n2}, M_{d2}$ on the positions of libration points, respectively. In Fig.1(a), we notice that the libration points are moving away from the origin as the value of R increases in the interval $[1, 3.5]$. We find that L1 has less movement compared to L4, L5. The displacement of L2, L3 is larger than L1, L3 and L4. In Fig. 1(b), we are decreasing the mass of galaxy G1 and increasing the mass of galaxy G2. We observe shifts in all libration points towards the negative direction of the x -axis. The shift of L1 is comparatively more than the shift of L2, L3, L4 and L5. Thus the parameters have a considerable impact on the position of libration points.

2.2. Zero-velocity curves

In the equation (9), if we take $\dot{x} = 0$ and $\dot{y} = 0$ then the expression $2\Omega - C = 0$ represents the zero-velocity curves. If we consider the expression $2\Omega - C \geq 0$ then it will represent the permissible region of motion where the movement of the charged particle take place.

In Fig. 4(a-f), the values of the fixed parameters are given. At these values, we find the position of all libration points. Five libration points ($L_i, i=1\dots 5$) are located. There are four different values of C_i 's corresponding to L_i 's (Jacobi integral) as C_4 and C_5 are equal. The values of C_i 's are $C_1 = 6.86825, C_2 = 6.5988, C_3 = 5.96756$ and $C_4 = C_5 = 5.22324$. We can divide the whole configuration space (x, y) into three parts: interior regions, outlying regions and forbidden regions of motion. There are five different cases:

- If $C > C_1$ then all necks are closed and therefore orbit can move around primaries or in outlying regions.

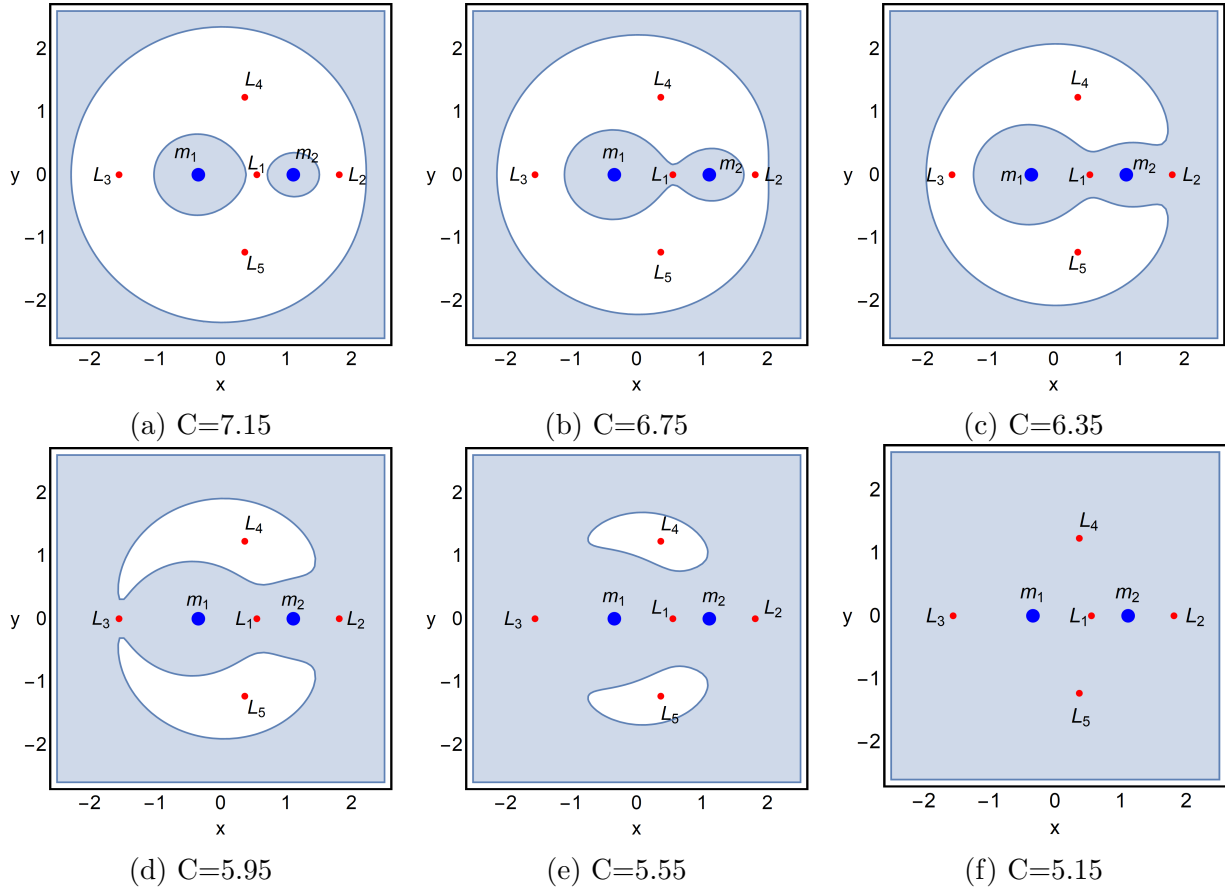


Fig. 2. Impact of variation of energy constant (Jacobi's Integral) on zero-velocity curves. Gray colour indicates region of motion. Blue color denotes the position of primaries m_1 and m_2 . The position of libration points are denoted by black dots. Other parameters have values $M_{n1} = 0.08$, $M_{d1} = 2.0$, $M_{n2} = 0.04$, $M_{d2} = 0.6$, $a_1 = 0.15$, $b_1 = 0.2542$, $h_1 = 0.00925$, $a_2 = 0.175$, $b_2 = 0.0789$, $h_2 = 0.00875$, $cn_1 = 0.0125$, $cn_2 = 0.01$, $R = 1.45$.

- When $C_2 < C \leq C_1$, no necks are open but interior regions around m_1 and m_2 get connected. Therefore motion is possible around both primaries, i.e., around interior regions or in exterior regions. However, the orbit can not escape from inner region to outer region or vice versa.
- When $C_3 < C \leq C_2$, one neck is open around m_2 allowing orbits to move close to m_2 and escape to exterior region.
- When $C_4 < C \leq C_3$, both necks are open; therefore, the movement of orbit can take place close to both primaries and escape to the outer region.
- When $C \leq C_4$, the orbit can move through the whole configuration space.

We have shown five different ((d) and (e) are of same cases) cases of zero velocity curves in Fig 2(a-f). In Fig. 2(a), we notice interior regions around m_1 and m_2 and also the exterior regions. The orbit can move near primaries and not around any libration points. In Fig. 2(b), we see that the interior regions around m_1 and m_2 get connected. So the orbit can move in the locality of primaries m_1 and m_2 . The orbit can also move around L_1 . In Fig. 2(c), there is one exit channel around m_2 and L_2 . Therefore the orbit can move close to m_1 and m_2 , and through exit channel, it can escape to outlying exterior regions. The movement of orbit is possible around L_1 and L_2 . Now, we decrease the value of C (Jacobi's integral) gradually. In Fig. 2(d), at the value of $C = 3.2$, there are two exit channels and also there are no forbidden regions around m_1 , m_2 , L_1 , L_2 and L_3 . Thus we notice the increase in the region of motion, but still, the motion is not possible around the triangular libration points. The same situation can be further observed in Fig. 2 (e). At the value $C = 5.15$, the forbidden region of motion vanishes completely. Therefore the orbit can move anywhere in the configuration space (x, y) (see Fig. 2 (f)). Thus, we observe a significant impact on the

geometry of zero-velocity curves due to variation of Jacobi's constant.

3. Newton-Raphson(NR)-BoA and Basin Entropy

3.1. *NR-BoA*

We can determine different aspects of the dynamical system with the help of the NR-BoA. In the recent past, just a few researchers have applied this method in various dynamical system including different disturbing terms in the effective potential (for e.g. [Zotos, 2018], [Suraj, 2019], [Zotos, 2017], [Kalvouridis et al., 2012], [Sprott et al., 2015] and their references). We use NR method (multivariate form) to study the BoA related to libration points. To reveal the domain of convergence for a particular libration point, we examine a set of initial conditions. To solve the systems of bivariate function $f(\mathbf{X}) = 0$, we apply the iterative scheme

$$\mathbf{X}_{n+1} = \mathbf{X}_n - J^{-1}f(\mathbf{X}_n),$$

where J is the Jacobian matrix of $f(\mathbf{X}_n)$.

In this work, the system of differential equations are given by

$$\begin{aligned}\Omega_x &= 0, \\ \Omega_y &= 0.\end{aligned}$$

With elementary calculations, we get the iterative formula for each coordinate as:

$$x_{n+1} = x_n - \left(\frac{\Omega_{x_n} \Omega_{y_n y_n} - \Omega_{y_n} \Omega_{x_n y_n}}{\Omega_{x_n x_n} \Omega_{y_n y_n} - \Omega_{x_n y_n} \Omega_{y_n x_n}} \right), \quad y_{n+1} = y_n + \left(\frac{\Omega_{x_n} \Omega_{y_n x_n} - \Omega_{y_n} \Omega_{x_n x_n}}{\Omega_{x_n x_n} \Omega_{y_n y_n} - \Omega_{x_n y_n} \Omega_{y_n x_n}} \right),$$

where x_n , and y_n are n -th step of the NR method. Partial derivatives of $\Omega(x, y)$ are given in the form of subscripts. The algorithm for computing BoA, we have applied the following steps:

- Initial conditions (x_0, y_0) are taken on the configuration plane (x, y) and apply NR method. In present calculations, we have adopted a grid of 1024×1024 initial conditions in an uniform way. These initial conditions are called nodes. The Min. and Max. values of x and y are chosen to view the complete picture of the BoA generated by the libration points.
- The method is applied continuously till an accuracy of order 10^{-15} or the maximum number of iterations (500) is reached for each initial condition. The stopping condition $|\mathbf{x}_{n+1} - \mathbf{x}_n| \leq 10^{-15}$ or $N \leq 500$ is used.
- For each initial condition, we record the number of iterations N to achieve the desired accuracy. For non-converging initial conditions, we further iterate for 10000 iterations using this method.
- We fix different colours for each libration point, and a particular colour is assigned to the initial conditions according to its convergence towards a specific libration point.
- After assigning all initial conditions one colour, we plot the colour coded graph, which is known as BoA. For all computations and simulations, we have used Mathematica 11.0 [Wolfram, 2017].

3.2. *Basin Entropy*

In 2016, A. Daza [Alvar, 2016] introduced a new tool to measure unpredictability of the basin of attraction. This new tool can quantify the uncertainty of BoA, known as basin entropy. We shall briefly discuss the algorithm for the computation of basin entropy:

- First of all, we complete the process of plotting BoA. In the configuration plane (x, y) , 1024×1024 initial conditions are taken, each having some colour as per its convergence towards libration points.
- In this step, we divide the whole region into different non-overlapping boxes to completely cover up the entire area. Each box contains precisely 25 trajectories. We have considered approximately 42000 non-overlapping boxes for this computation.

Table 1. Number of initial conditions converging towards different libration points and the values of entropy S_b and S_{bb} due to variation in parameter R .

R	Total Points	L1	L2	L3	L4	L5	Execution time	S_b	S_{bb}
1.0	1003072	453456	10797	69495	234662	234662	2029.3	0.923136	1.07934
1.5	1047741	465262	107185	17873	228770	228651	2809.01	0.884452	1.10743
2.0	1051051	499101	97712	20272	216922	217044	3539.67	0.806377	0.930766
2.5	1046999	522472	104492	18384	200762	200889	3161.13	0.881633	0.991321
3.0	1024382	486481	98751	20294	209429	209427	2149.5	0.919124	1.0552
3.5	1012300	476105	104206	19413	206381	206195	3410.12	0.940689	1.07509

- We compute the probability of colour j inside each box i denoted as p_{ij} . The gibbs entropy for each box i is computed as

$$S_i = \sum_{j=1}^{m_i} p_{ij} \log \left(\frac{1}{p_{ij}} \right), \quad (10)$$

where $m_i \in [1, N_A]$ is the number of colours inside the box i and N_A represents the number of libration points. The probabilities p_{ij} are calculated as

$$p_{ij} = \frac{\text{number of trajectories leading to colour } j}{\text{number of trajectories in the box } i}.$$

- Eventually, due to selection of non overlapping boxes N , the entropy of the whole grid is equal to the summation of entropy of each box i of the grid.

$$S = \sum_{i=1}^N S_i = \sum_{i=1}^N \sum_{j=1}^{m_i} p_{ij} \log \left(\frac{1}{p_{ij}} \right).$$

Now, we define the basin entropy as

$$S_b = \frac{S}{N}.$$

In similar way, we define boundary basin entropy as

$$S_{bb} = \frac{S}{N_b}.$$

where N_b denotes the number of boxes having more than one colour.

If the values of S_b and S_{bb} are greater than $\log 2$, the BoA or boundaries along BoA is fractal in nature. Now, we study the effect of the parameters $R, M_{n1}, M_{d1}, M_{n2}$ and M_{d2} on the BoA. We have considered two cases: In first case, the effect of parameter R and in the second case, effect of parameters M_{n1}, M_{d1}, M_{n2} and M_{d2} .

4. Effect of parameters R & M_{n1}, M_{d1}, M_{n2} and M_{d2} on the BoA

4.1. Influence of R (distance between center of two galaxies)

We begin our investigations with the case, where R varies in the interval $[1, 3.5]$ and we take $M_{n1} = 0.08, M_{d1} = 2.0, M_{n2} = 0.04$ and $M_{d2} = 0.6$. In Fig. 3, the BoA for libration points are depicted by five different colours. Also, the BoA cover all of the configuration plane (x, y) . Most importantly, we notice that a slight change in the value of the parameter R , the geometry of the basins changes significantly. In particular, the change in Fig. 3 (a) to Fig. 3(b) can be seen. Here the region of liberation point L5 (green) in the upper part of Fig. 3 (a) shrunk significantly in Fig. 3 (b) due to little change in the value of R . A similar observation can be seen for the basin corresponding to liberation point L4 (pink) in the bottom of the figures. When the value of R is changing from 1 to till 3.5, a major change is observed in Fig. 3(a) to Fig. 3 (f). Despite having the same number of initial conditions converging towards L4 and L5, there is a regular change in the shape of BoA for different values of R . The domain of convergence of libration

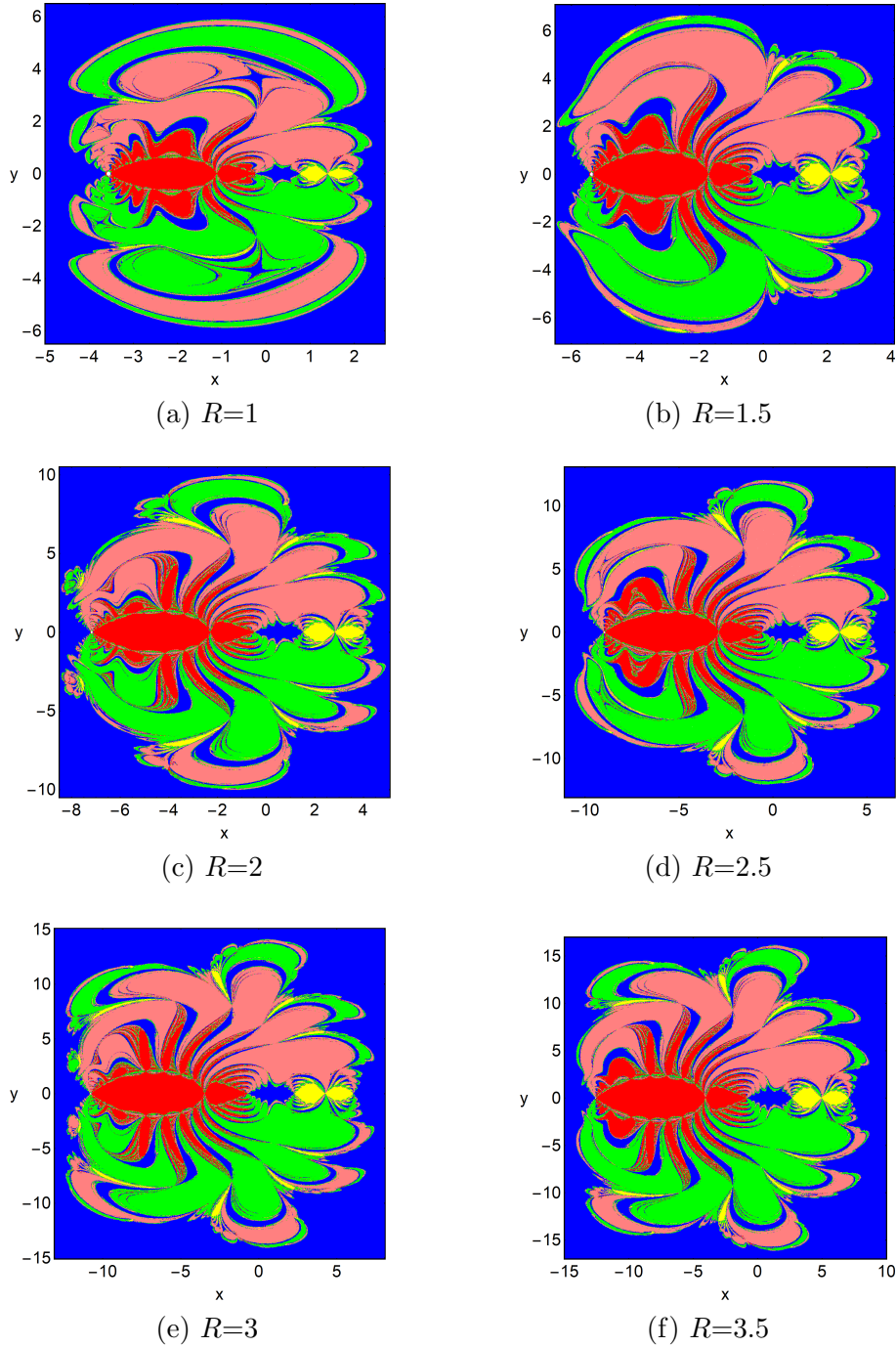


Fig. 3. BoA for different values of R . The colour codes for the BoA related to libration points are L1 (blue), L2 (Red), L3 (Yellow) , L4 (Pink) and L5 (Green).

point L1 extends towards infinity whereas the domain of convergence due to libration points L2, L3, L4 and L5 is finite for such values of R . Further, we observe that basins for libration points L2 and L3 have the shape like insect with legs and antennas. Also, the shape of BoA corresponding to libration points L4 and L5 appears as many wings of a butterfly. In Fig. 4 (a-f), we have shown Pie-Chart for the number of iterations needed for all initial conditions taken in the configuration plane (x, y) . In Fig. 4 (a), it is clear that the maximum number of iterations needed are 8, 9 and 10 ($8 \rightarrow 229994, 9 \rightarrow 213628, 10 \rightarrow 163375$). Likewise, we have recorded the number of iterations taken by initial conditions to converge for different values of R . We notice that approximately 95 % of the initial conditions converge after 25 iterations. A

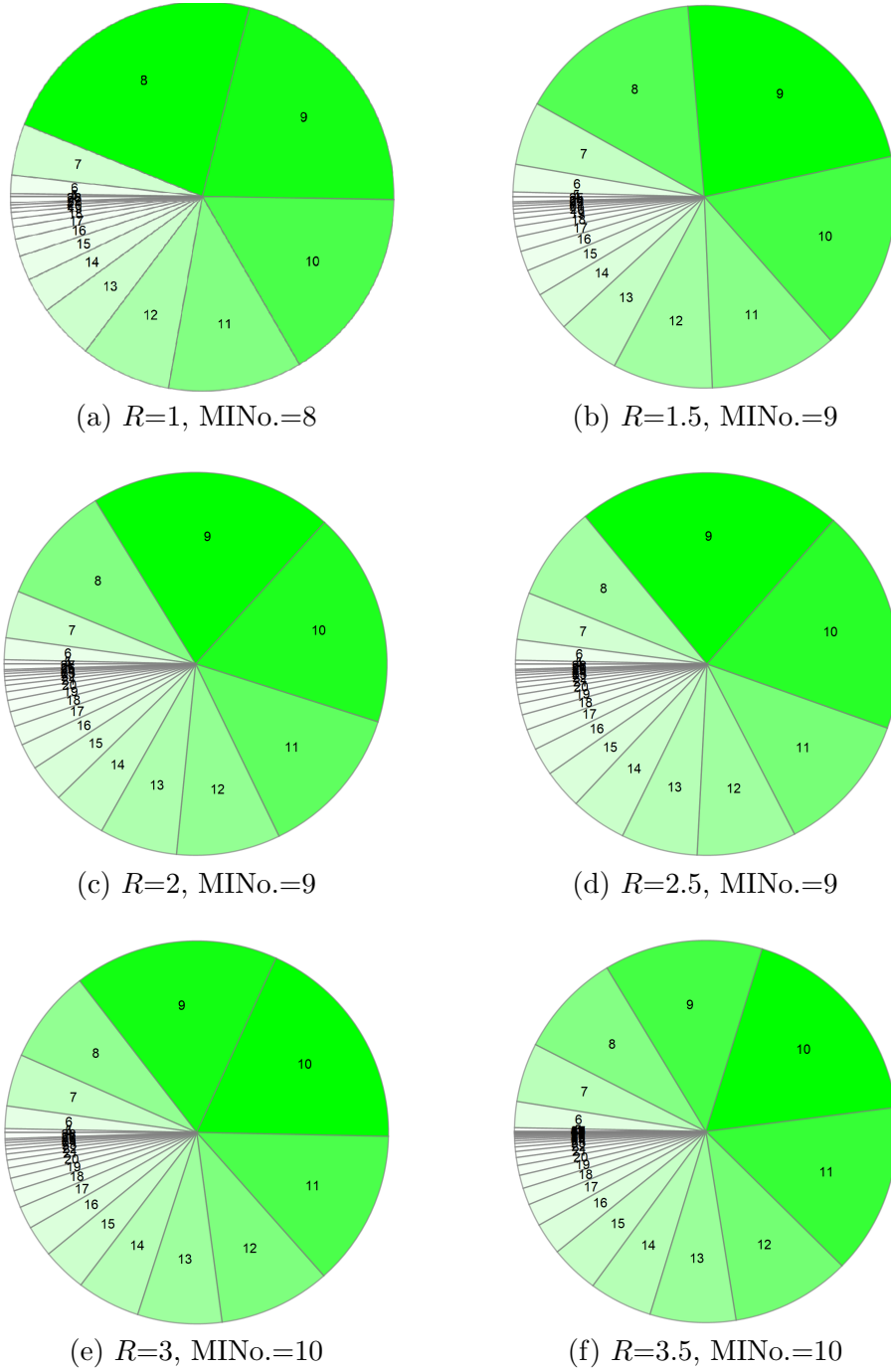


Fig. 4. (a-f) Pie-chart of number of required iterations for different values of R . MINo. denotes the maximum number of iterations.

maximum number of initial conditions converge after 8 to 10 number of iterations.

In Fig. 5 (a-f) the relationship between numbers of iterations needed and the initial conditions considered in the configuration plane (x, y) has been established. The blue tone is used to represent the iterations needed for each initial condition. We notice that the initial conditions along the boundaries of the basins require more iterations than other initial conditions. In Table 1, we have mentioned the details of convergence of initial conditions towards the libration points L1, L2, L3, L4 and L5. The value of basin entropy S_b and boundary basin entropy S_{bb} is also given in Table 1 for different values of R . Based on Table 1, Fig. 3, Fig. 4 and Fig. 5, we sum up the following things:

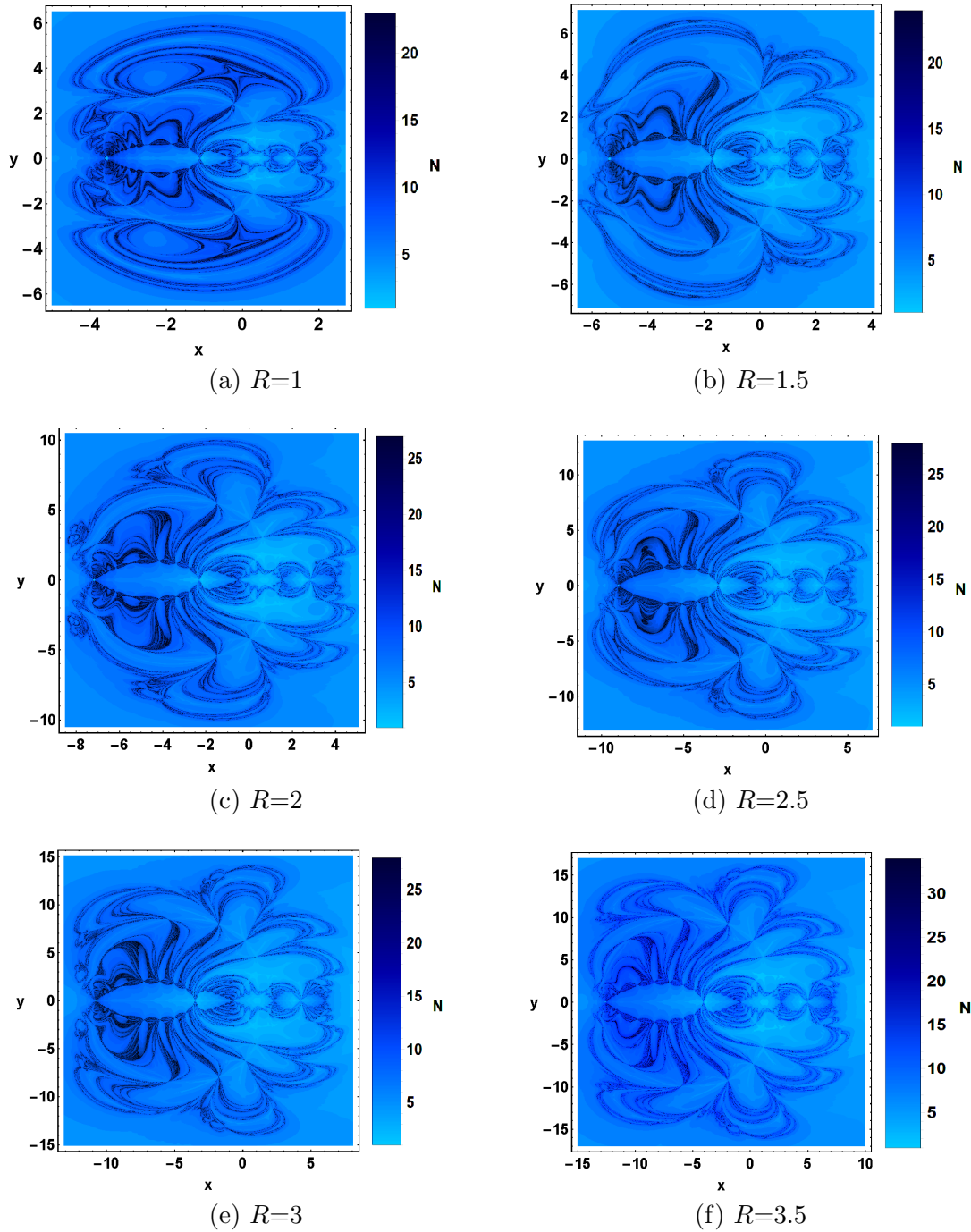


Fig. 5. (a-f) Iterations N (blue tone) required to achieve desired accuracy for different values of R .

- Due to changes in the value of R , if we move from Fig. 3(a) to Fig. 3(f), we observe a significant change in the geometry of BoA.
- The region occupied by the initial conditions converging towards L_4 and L_5 are approximately equal for each case, although their geometry is changing in every case (see Table 1).
- In all cases, the maximum number of iterations required for the convergence of 95% of the initial conditions are below 25. To achieve the desired accuracy, i.e. of order 10^{-15} , the maximum probable number of iterations lies between 8 to 10 (See Fig. 4(a-f)).
- From Table 1, we see that the value of basin entropy S_b and boundary basin entropy S_{bb} is greater than $\log(2)$ and therefore the existence of fractal is verified. The value of boundary basin entropy S_{bb} is higher

than the entropy of other regions indicates the existence of higher fractal regions along the boundaries. From Table 1 and Fig. 5, we conclude that the initial conditions which lie within the fractal regions require more iterations to converge.

4.2. Influence of M_{n1} , M_{d1} , M_{n2} and M_{d2}

Table 2. Number of initial conditions converging towards different libration points and the values of entropy S_b and S_{bb} due to variation in parameters M_{n1} , M_{d1} , M_{n2} and M_{d2} . $R=2$ is fixed.

$M_{n1}, M_{d1}, M_{n2}, M_{d2}$	Total Points	L1	L2	L3	L4	L5	Execution Time	S_b	S_{bb}
0.08, 2.0, 0.04, 0.6	1012300	476105	104226	19413	206381	206195	2368.86	0.806377	0.930766
0.06, 1.8, 0.06, 0.8	1043359	477939	93673	28561	221538	221648	2628.81	0.941639	1.06536
0.04, 1.6, 0.08, 1.0	1073073	595431	63702	30089	191832	192019	1812.15	0.861113	0.985576
0.02, 1.4, 0.1, 1.2	1037341	532105	46465	42676	208134	207961	2552.17	0.661595	0.882299
0.01, 1.2, 0.12, 1.4	1011026	482757	37538	60105	215528	215098	3539.01	0.970159	1.05315
0.008, 1.0, 0.14, 1.6	1020700	527815	27792	72293	196344	196456	2429.71	0.948648	1.06536

We continue our investigations with another case where the masses of a nucleus M_{n1} and the disk M_{d1} of a galaxy (G1) is decreasing and the masses of nucleus M_{n2} and the disk M_{d2} of galaxy G2 is increasing. We have displayed BoA for six values in Fig. 6(a-f). In all cases, the value of $R = 2$ is fixed. In Fig. 7(a-f), the Pie-chart related to different parameters is displayed. Fig.8(a-f) comprises of the different graphs representing the iterations needed for each initial conditions.

Further, in Fig. 6(a-f), we notice that the BoA for L2 is decreasing, and for L3, it is increasing due to variation in parameters. We observe in Fig. 6(a) few small regions in the left part which disappeared in the next Fig. 6(b) due to change in parameters. We notice such changes or other when we move from Fig. 6(a) to Fig. 6(f). Similar to the previous case, the BoA corresponding to L1 extends to infinity. The BoA of L4 and L5 remain more or less the same in all cases. The shape of BoA of libration points L4 and L5 looks like many butterfly wings. We also observe that the BoA of libration points L2 and L3 have the shape like insects with legs and antennas.

Similar to Table 1, Table 2 comprises the number of initial conditions converging towards different libration points. The value of basin entropy and boundary basin entropy is also given in Table 2. By Table 2, it is evident that the almost entire region in the BoA (except one case) is fractal. The value of S_{bb} is more than the value of S_b indicates the presence of more fractal regions along the boundaries.

The number of iterations needed for convergence towards libration points for all initial conditions varies from 5 to 30. The distribution of iterations is shown using Pie-chart in Fig. 7 (a-f). The maximum probable iterations are 7 or 8 or 9 in almost all cases. Similar to the case I, 95% initial conditions converge in 25 iterations. The number of iteration needed to convergence for each initial condition is displayed in Fig. 8(a-f). The number of required iterations is presented using a blue tone, i.e., deep blue tone represents more iteration than faded blue tone. This figure gives us a clear idea of the regions where there is a need for more number of required iterations. We summaries followings from Table 2, Fig. 6, Fig. 7 and Fig. 8.

- The total area covered by BoA corresponding to L2, L3, L4 and L5 are finite whereas the area covered by a BoA of libration point L1 extends to infinity. The configuration plane (x, y) is filled by BoA completely.
- All initial conditions are converging towards one of the five libration points with the accuracy 10^{-15} . We do not find any non-converging points.
- Except for one value of a parameter, the existence of fractal is verified by the values of basin entropy given in Table 2. However, in this particular case, the boundaries of BoA are fractal. In all other cases, there is a presence of highly fractal regions along the boundaries (See Table 2 and Fig. 8(a-f)).
- In all cases, the maximum number of iterations needed for the convergence of 95% of the initial conditions are below 15. The maximum probable number of iterations needed to achieve the desired accuracy lies between 7 to 10.

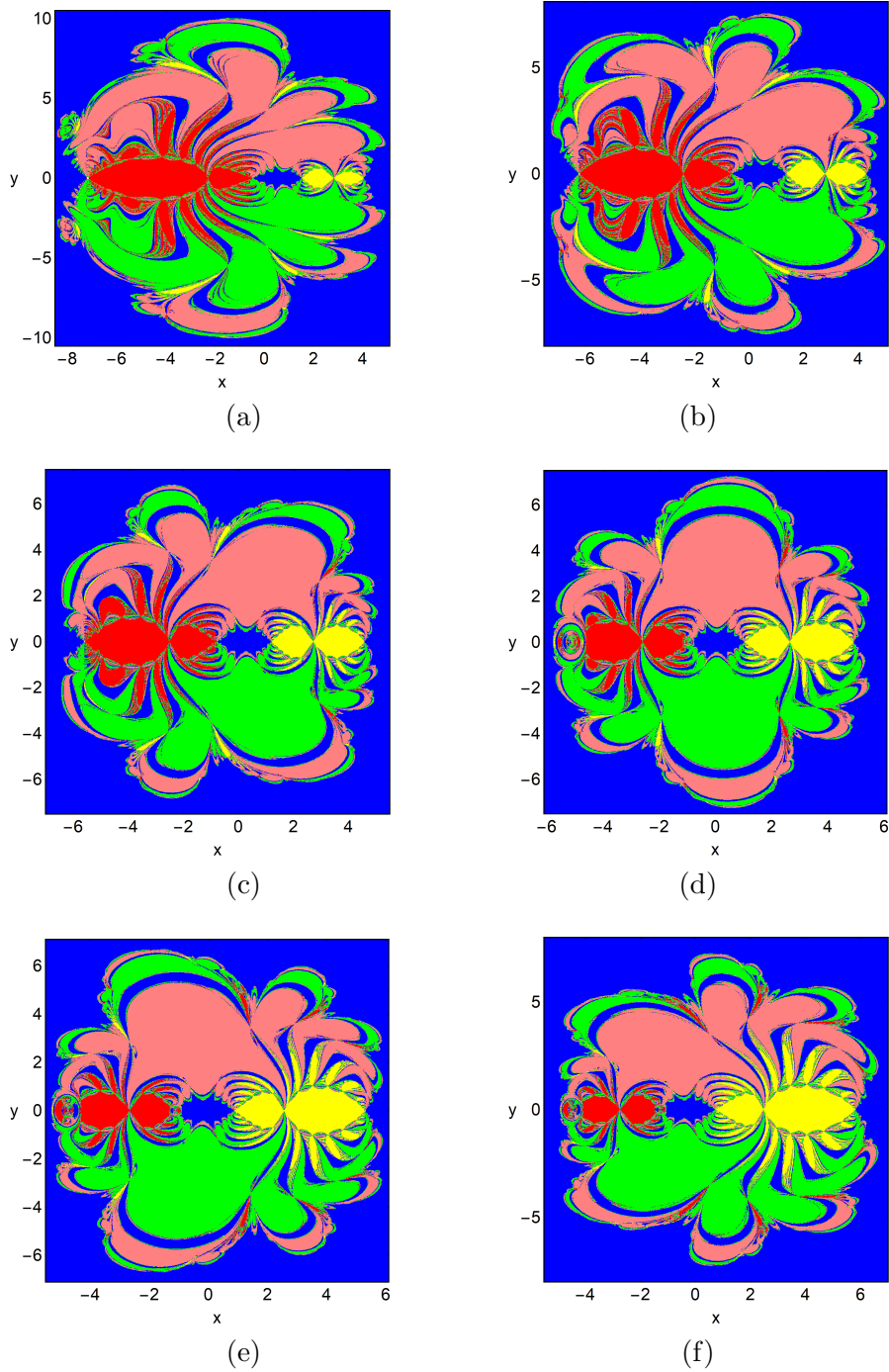


Fig. 6. BoA for different values of M_{n1} , M_{d1} , M_{n2} and M_{d2} . The colour codes for the BoA corresponding to libration points are L1 (blue), L2 (Red), L3 (Yellow), L4 (Pink) and L5 (Green). The different values of the parameters are (a) $M_{n1} = 0.08$; $M_{d1} = 2.0$; $M_{n2} = 0.04$; $M_{d2} = 0.6$; (b) $M_{n1} = 0.06$; $M_{d1} = 1.8$; $M_{n2} = 0.06$; $M_{d2} = 0.8$; (c) $M_{n1} = 0.04$; $M_{d1} = 1.6$; $M_{n2} = 0.08$; $M_{d2} = 1$; (d) $M_{n1} = 0.02$; $M_{d1} = 1.4$; $M_{n2} = 0.1$; $M_{d2} = 1.2$; (e) $M_{n1} = 0.01$; $M_{d1} = 1.2$; $M_{n2} = 0.12$; $M_{d2} = 1.4$; (f) $M_{n1} = 0.008$; $M_{d1} = 1.0$; $M_{n2} = 0.14$; $M_{d2} = 1.6$. $R=2$ is fixed.

5. Concluding Remarks

The novelty and importance of this work are clear from the fact that we have chosen this model for the first time to study the BoA and the measure of uncertainty involved in it. Besides this, we have investigated the existence of fractal regions in BoA. The binary system of interacting galaxies has been explored in the framework of the Circular Restricted Three-Body Problem. The parametric evolution of libration points is

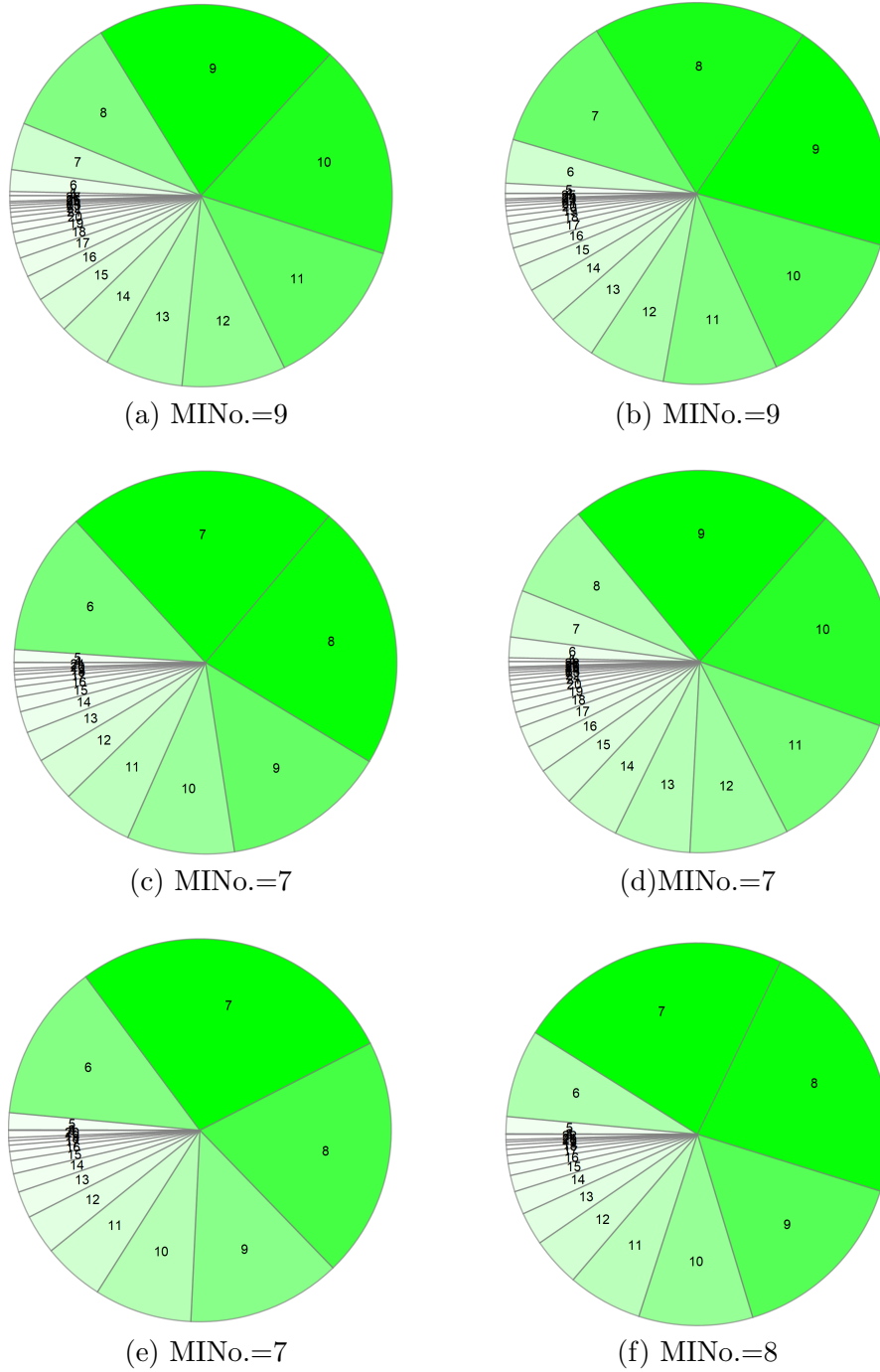


Fig. 7. (a-f) Pie-chart of number of iterations taken (N) for different values of M_{n1} , M_{d1} , M_{n2} and M_{d2} . The different values of the parameters are (a) $M_{n1} = 0.08$; $M_{d1} = 2.0$; $M_{n2} = 0.04$; $M_{d2} = 0.6$; (b) $M_{n1} = 0.06$; $M_{d1} = 1.8$; $M_{n2} = 0.06$; $M_{d2} = 0.8$; (c) $M_{n1} = 0.04$; $M_{d1} = 1.6$; $M_{n2} = 0.08$; $M_{d2} = 1$; (d) $M_{n1} = 0.02$; $M_{d1} = 1.4$; $M_{n2} = 0.1$; $M_{d2} = 1.2$; (e) $M_{n1} = 0.01$; $M_{d1} = 1.2$; $M_{n2} = 0.12$; $M_{d2} = 1.4$; (f) $M_{n1} = 0.008$; $M_{d1} = 1.0$; $M_{n2} = 0.14$; $M_{d2} = 1.6$. $R=2$ is fixed. MINo. denotes the maximum number of iterations.

shown in Fig. 1. The impact of Jacobi's constant on the geometry of zero-velocity curves is shown in Fig. 2. The multivariate form of the NR method is used to find the convergence of initial conditions towards libration points (act as attractors in the present case). With the help of shape of basins, the influence of parameters R and M_{n1} , M_{d1} , M_{n2} , M_{d2} is analysed (Fig. 3 and 5). The data obtained from numerical simulations is given in Table 1 and Table 2, which reflects the originality of this work. Table 1 and Table 2 comprises of the details convergence of initial conditions towards libration points; time consumed by CPU;

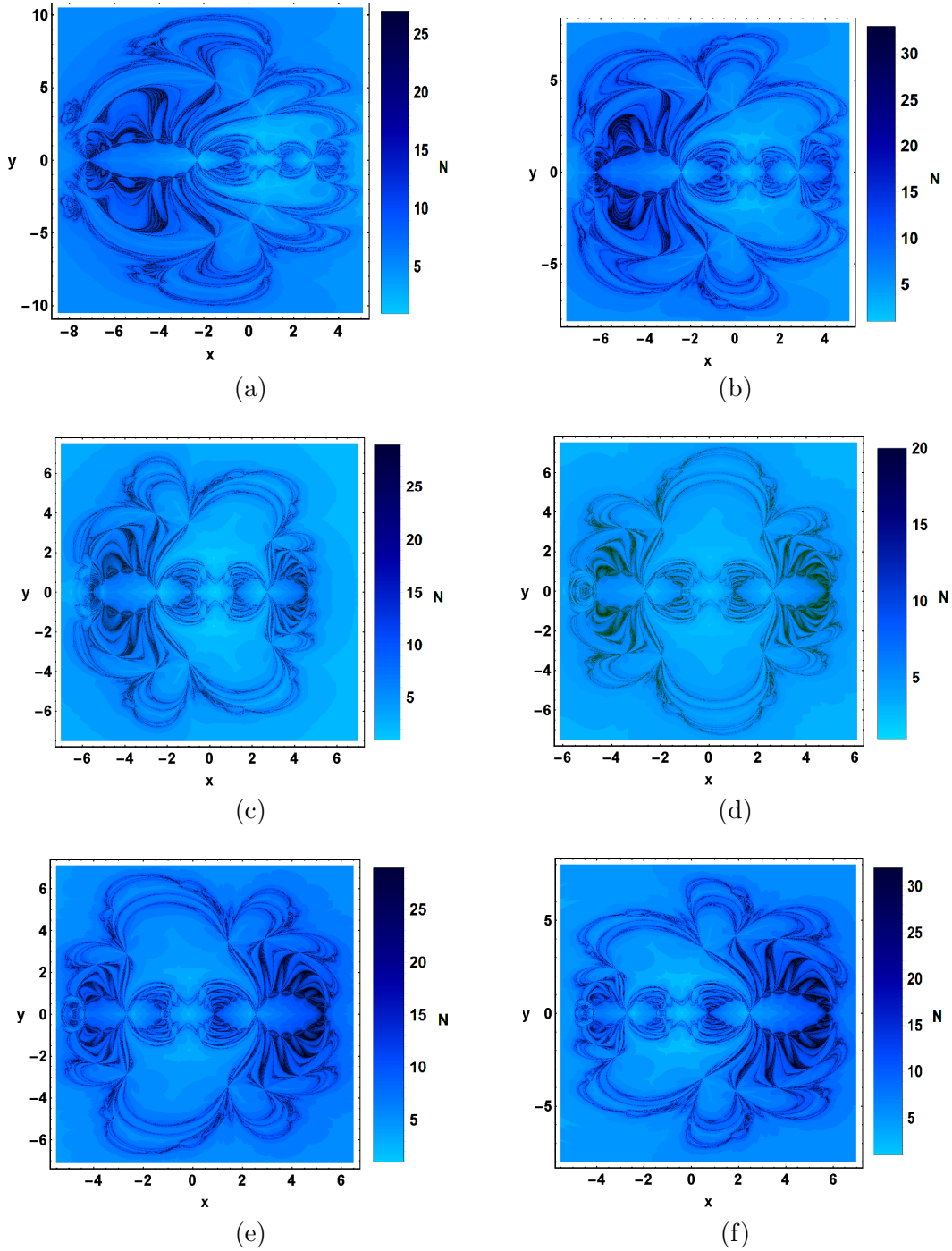


Fig. 8. (a-f) Iterations N (blue tone) needed to achieve desired accuracy for different values of M_{n1} , M_{d1} , M_{n2} and M_{d2} . The different values of the parameters are (a) $M_{n1} = 0.08$; $M_{d1} = 2.0$; $M_{n2} = 0.04$; $M_{d2} = 0.6$; (b) $M_{n1} = 0.06$; $M_{d1} = 1.8$; $M_{n2} = 0.06$; $M_{d2} = 0.8$; (c) $M_{n1} = 0.04$; $M_{d1} = 1.6$; $M_{n2} = 0.08$; $M_{d2} = 1$; (d) $M_{n1} = 0.02$; $M_{d1} = 1.4$; $M_{n2} = 0.1$; $M_{d2} = 1.2$; (e) $M_{n1} = 0.01$; $M_{d1} = 1.2$; $M_{n2} = 0.12$; $M_{d2} = 1.4$; (f) $M_{n1} = 0.008$; $M_{d1} = 1.0$; $M_{n2} = 0.14$; $M_{d2} = 1.6$. $R=2$ is fixed.

the value of basin entropy and boundary basin entropy. The number of iterations needed for the convergence of the initial conditions is shown using Pie-chart (in the tone of green colour) in Fig. 4 and Fig. 7, which is useful, informative and different from earlier works. Further, we have established the relationship between the number of iterations required for convergence and the set of initial conditions on configuration plane (x, y) (Fig. 5 and 8).

For all numerical simulations, we have used a machine configured with Intel(R) Core(TM) i7-8550U

CPU 1.80 GHz. In all cases, the computational time of the CPU is less than or equal to one hour for the simulation a uniform grid of 1024×1024 initial conditions (nearly ten lakhs). The time taken by the CPU to classify all initial conditions is less than one minute. We have considered six different values of all the parameters. The results of simulations can be summarized as follows:

- The programming for the computation of BoA; basin entropy and plotting of all graphs is done on Mathematica. The execution time taken by CPU for BoA and the classification of initial conditions in this model is explicitly mentioned in Table 1 and Table 2. As per data available from earlier works, the time mentioned in Table 1 and Table 2 is comparatively less.
- In almost all cases, we find that configuration plane (x, y) contains the combinations of fractal regions and distinct BoA. If we choose an initial condition in these regions, it is challenging to predict the convergence towards a specific libration point. The unpredictability of basin of attraction is due to the non-linearity of the expressions of the potential responsible for the motion of a star in the presence of the two interacting galaxies (G1 and G2) (See equation (4)). These regions are mainly located along with the neighbourhood of boundaries of BoA.
- The area enclosed by BoA corresponding to libration points L2, L3, L4 and L5 are finite whereas, the area associated with central libration point L1 extends to infinity. Also, the area of basins corresponding to L4 and L5 are approximately the same for all cases. The area of basins corresponding to L2 and L3 changes due to variation in the parameters.
- Based on simulations, we observe that all the initial conditions (10 lakhs approx.) on a uniform grid of 1024×1024 converge to any one of the five libration points of the dynamical system with an accuracy of order 10^{-15} . We do not find any non-converging initial condition. (See Table 1 and Table 2)
- Fig. 5 (a-f) and Fig. 8 (a-f) reveal that all initial conditions which require more iterations lie along the boundaries of BoA, i.e., along with the fractal regions as compare to Initial conditions lying away from boundaries.
- Due to a decrease in the mass of the galaxy (G1) and the increase of the mass of the galaxy (G2), the area of a BoA due to L2 decreases and the area of a BoA due to L3 increases. However, the region occupied by BoA due to L4 and L5 is roughly the same for all cases. (See Fig. 6 (a-f))
- By Table 1 and Table 2, we find that the values of entropy S_b and S_{bb} is greater than $\log 2$ except for one value of S_b in Table 2. Thus all BoA are fractal and there is an existence of highly fractal regions along the boundaries.
- The maximum number of iteration that an initial condition needs to converge towards libration points lie between 7-10 for all cases. (See Fig. 4 (a-f) and Fig. 7 (a-f)).
- The parameters have a significant impact on the evolution of libration points as well as the geometry of zero-velocity curves.

We observe very few research works in the area of space dynamics. That is why we have considered a galactic model for our work. These results will be useful for many researchers to work in these models. On the other hand, these observations give us an intuitive idea for the existence of some properties (like a different type of basins, the existence of Wada basin). In future, we will try to investigate these properties in other complex nonlinear models in the field of space dynamics and celestial mechanics.

References

- Daza, Alvar et al. [2016], Basin entropy: a new tool to analyze uncertainty in dynamical systems. Scientific Reports, **6**, 31416.
- Daza, Alvar et al. [2017], Chaotic dynamics and fractal structures in experiments with cold atoms, Phys. Rev. A **95**, 013629.
- Daza, Alvar et al. [2018], Basin Entropy, a Measure of Final State Unpredictability and Its Application to the Chaotic Scattering of Cold Atoms, Chaotic, Fractional, and Complex Dynamics: New Insights and Perspectives. Understanding Complex Systems, 9-34.
- Hasan, H., Pfenniger, D. and Norman, A. C. [1993], Galactic bars with central mass concentrations three-dimensional dynamics, APJ, **409**, 91.

- Kalvouridis, T. and Gousidou-Koutita, M. [2012], Basins of Attraction in the Copenhagen Problem Where the Primaries Are Magnetic Dipoles, *Applied Mathematics*, **3**, 6, 541-548.
- Kumar, Vinay, Gupta, Beena R & Aggarwal, R. [2016], Numerical Investigation of a Star's Trajectory in Binary Quasar System, *Advanced Studies in Contemporary Mathematics*, **26**, 3.
- Latewe, G., Magain, P., and Courbin, F. et al. [2007], On-axis spectroscopy of the host galaxies of 20 optically luminous quasars at $z \approx 0.3$, *MNRAS*, **378**, 1, 83-108.
- Miyamoto, W. and Nagai, R. [1975], Three-dimensional models for the distribution of mass in galaxies, *PASJ*, **27**, 533.
- Sillanpaa, A., Haarala, S. and Valtonen, M. J. [1988], OJ 287- Binary pair of supermassive black holes, *APJ*, **325**, 628.
- Sprott, J. C. and Xiong, A. [2015], Classifying and quantifying basin of attraction, *Chaos: An Interdisciplinary Journal of Nonlinear Science*, **25**, 8.
- Wolfram Research, Inc. [2014], *Mathematica*, Version 11.0.1, Champaign, IL.
- Sanam Suraj, Md., Sachan, Prachi., Zotos E. E., Mittal, A., Aggarwal, R., [2019], On the NewtonRaphson basins of convergence associated with the libration points in the axisymmetric restricted five-body problem: *Int. J. Non-Linear Mech.*, **112**, 25-47.
- Zotos., E. E. [2012], Order and chaos in three dimensional binary system of interacting galaxies, *APJ*, **750**, 56.
- Zotos, E. E. [2017a], Revealing the basins of convergence in the planar equilateral restricted four-body problem. *Astrophys. Space Sci.* **362**, 2.
- Zotos E. E., Kumar Satya S., Aggarwal, R. and Sanam Suraj, M. [2018], Basins of Convergence in the Circular Sitnikov Four-Body Problem with Nonspherical Primaries, *Int. J. of Bifurcation and Chaos*, **28**, 05, 1830016.